in the foregoing) appears to be a reasonable choice for a bluntness parameter, since it is completely specified by the bow shock, which, in turn, is governed by the body shape For the data under consideration, it appears that the square of this Mach number ratio may be used to collapse all the data into one grouping, as shown in Fig 4 The correlation is of the form $(R_{x_{TR}})_\infty(M_\infty/M)^2$ as a function of M_∞, where the local Mach number M is obtained as just described It is seen that this correlation represents all the data, at least to first order

Figure 3 shows X_{TR}/d as a function of the inverse local Reynolds number based on body diameter, $(R_d)^{-1}$ Here, the effect of Mach number and body bluntness (cones vs spheres) is re-emphasized The fact that the sphere data do not group with the cone data on the basis of local Mach number supports the concept of a constant $(R_{ex_{TR}})_e$ for spheres

The sphere-cone data are shown in Fig 3 according to data reduction both as a cone and as a sphere The "sphere-cone as a cone" correlates much better with the cone data than does the "sphere-cone as a sphere" with the sphere data This may be partially explained by the fact that, for the experimental conditions, boundary-layer calculations indicate that the boundary layer on this blunt sphere-cone "swallows" a substantial portion of the fluid that passes through the strongest region of the bow shock Consequently, the inviscid wake fluid has not passed through a normal shock but rather through a weaker shock; therefore, it is representative of the inviscid flow associated with a slender vehicle

Additional information relating to the "sticking distance"[7] may be deduced from Fig 3 However, lack of space precludes an extensive discussion here; it is only noted that the correlation used by Demetriades[8] which employs the difference between transition and "sticking" distances in the Reynolds number does not improve any of the correlations shown here (In some cases, scatter is actually increased) Further details on this point and on other aspects of the material presented here may be found in Ref 11

References

[1] Slattery, R E and Clay, W G, The turbulent wake of hypersonic bodies," ARS Preprint 2673 62 (November 1962)

[2] Slattery, R E and Clay, W G, 'Laminar turbulent transition and subsequent motion behind hypervelocity spheres," ARS J 32, 1427–1429 (1962)

[3] Pallone, A J, Erdos, J I Eckerman, J, and McKay, W, "Hypersonic laminar wakes and transition studies," IAS Preprint 63-171 (June 1963)

[4] Demetriades, A "Hot-wire anemometer measurements in a hypersonic wake," *Proceedings of the 1961 Heat Transfer and Fluid Mechanics Institute* (Stanford University Press, Stanford, Calif, 1961)

[5] Demetriades, A, 'Hot wire measurements in the hypersonic wakes of slender bodies, AIAA Preprint 63-444 (August 1963)

[6] Webb, W H, Hromas, L, and Lees, L, 'Hypersonic wake transition," AIAA J 1, 719–721 (1963)

[7] Lees, L, "Hypersonic wakes and trails," ARS Paper 2662-62 (November 1962)

[8] Demetriades, A and Gold, H, Transition to turbulence in the hypersonic wake of blunt bluff bodies" ARS J 32, 1420–1421 (1962)

[9] Chapman, D R Kuehn, D M, and Larson, H K, "Investigation of separated flows in supersonic and subsonic streams with emphasis on the effect of transition,' NACA Rept 1356 (1958)

[10] Larson, H K, "Heat transfer in separated flows, J Aerospace Sci 26, 731–738 (1959)

[11] Zeiberg S L, "Correlation of hypersonic wake transition data," General Applied Sci Labs TR 382 (October 1963)

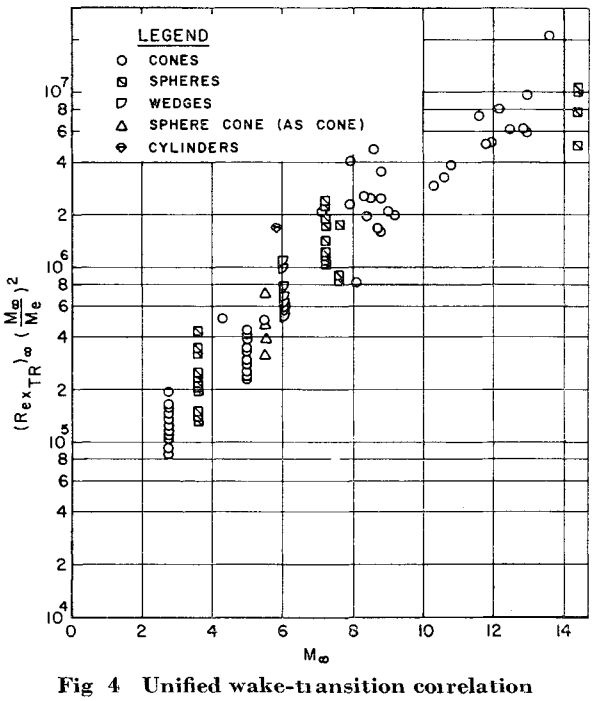

Fig 4 Unified wake-transition correlation

Approximate Nonequilibrium Air Ionization in Hypersonic Flows over Sharp Cones

E S Levinsky* and F L Fernandez†
Aerospace Corporation, San Bernardino, Calif

SEVERAL highly accurate methods have recently been developed for obtaining the nonequilibrium electron density distribution about a sharp re entering body Thus, Wood et al [1] have obtained inviscid flow-field solutions for cones and ogives by coupling the method of characteristics with a chemically reacting streamtube analysis between grid points

For the multicomponent air laminar boundary layer, numerical solutions of the coupled boundary layer and chemical kinetic equations have been obtained by Lenard and Blottner[2] by a finite difference method and by Pallone et al [3] using a multistrip integral approach These procedures, in general, are quite accurate but require extensive use of high-speed digital computers

More approximate boundary-layer theories that have been used are the "streamtube" method, which neglects diffusion, e g, DeRienzo et al [4] and Pallone et al,[3] and the method of "local similarity," e g, Lenard and Blottner [2] The streamtube procedure, although highly flexible and useful for assessing effects of different chemical reactions, overpredicts the ionization rates The locally similar method[2] involves the solution of a nonlinear two-point boundary-value problem and requires more computer time than the more accurate finite-difference method, especially at the larger distances from the nose Thus, Blottner[5] concludes that, even for the two-component case (dissociating oxygen), the finite-difference method is more efficient

Received November 4, 1963; revision received December 4, 1963 Supported by Ballistics Systems Division, U S Air Force under Air Force Contract No AF 04(695)-269

* Head, Gasdynamics Section, Engineering Division Associate Member AIAA

† Member of the Technical Staff, Engineering Division

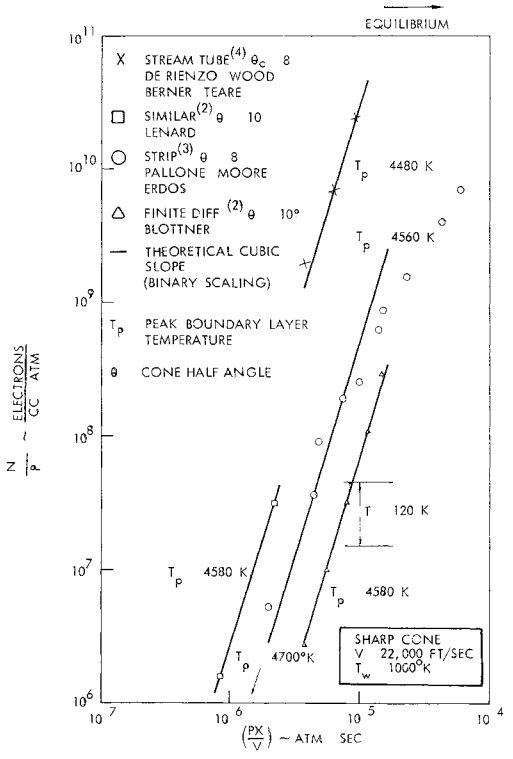

Fig 1 Comparison of nonequilibrium boundary-layer theories

The nonequilibrium boundary-layer analysis to be developed in the present paper is also based on local similarity However, a simplified model for the ionization kinetics of air together with the use of the frozen temperature distribution, as a first approximation, allows the continuity of species equations to be decoupled and linearized Their integration is thereby reduced to the matter of a simple quadrature of known functions, permitting the procedure to be used for parametric studies A comparison with results of the more accurate theories is presented Additional calculations are given in Ref 6

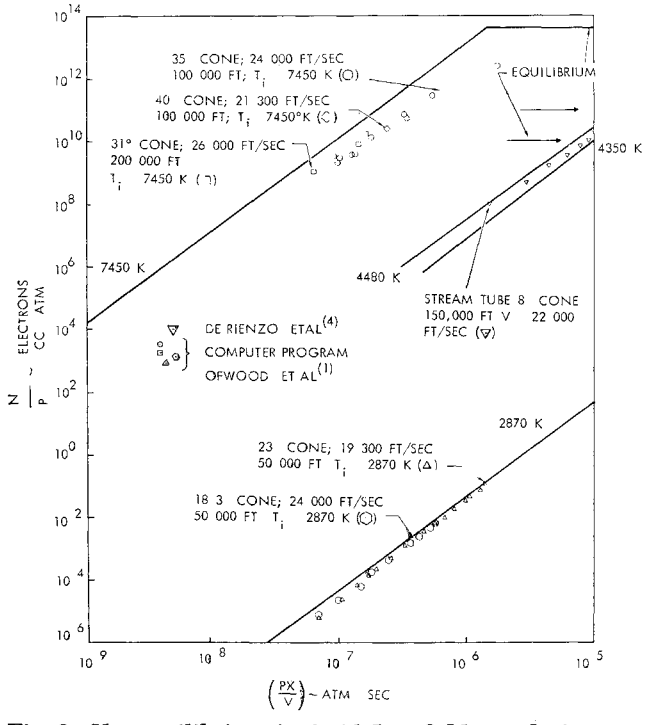

Fig 2 Nonequilibrium inviscid flow-field correlation

Correlations of Available Boundary-Layer Solutions

Figure 1 presents the variation of the peak value of n/P as a function of the parameter PX/V for the results from Refs 2–4, where n_e is the electron number density per cubic centimeter, P is the cone surface pressure in atmospheres, X is the distance from the vertex, and V is the surface velocity The parameter PX/V for a fixed temperature is essentially the binary scaling parameter discussed by Gibson and Marrone [7] The higher levels of the "streamtube" and "locally similar" results should be noted The difference between the "finite-difference" and "multistrip" integral methods can be explained, at least in part, as resulting from extreme sensitivity of peak n_e/P to the higher peak temperature as calculated by the latter method This may be due to different assumptions pertaining to the transport properties, which are difficult to evaluate

It is also of interest that all the data have a cubic slope, $n/P \sim (PX/V)^3$, up to about two decades below equilibrium This cubic law can be predicted on the basis of a simplified kinetic model for ionized air, as long as recombination, reattachment, and dissociative cooling can be neglected

Simplified Ionization Kinetics

The following chemical reactions are usually considered for ionizing air, e g., Wray[8]:

$$\begin{aligned} O_2 + M &\rightleftharpoons 2O + M \\ O + N_2 &\rightleftharpoons NO + N \\ N + O_2 &\rightleftharpoons NO + O \\ N + O &\rightleftharpoons NO^+ + e^- \\ N_2 + M &\rightleftharpoons 2N + M \\ N_2 + O_2 &\rightleftharpoons 2NO \\ N + O + M &\rightleftharpoons NO + M \end{aligned}$$

Only the first four reactions are used here It is assumed that the remaining reactions are either much slower or, as in the case of the sixth reaction, thermally and kinetically unimportant Only the forward reactions are considered, and depletion of the reacting molecular species is neglected

A chain reaction is assumed with the first reaction producing atomic oxygen from an Arrhenius-type law at the rate

$$\omega_O/\rho = \rho k_1^F(\tfrac{9}{32}C_{O_2} + \tfrac{2}{28}C_{N_2})C_{O_2}$$

where ω_O is the mass production rate of atomic oxygen per unit volume, ρ is the density, k_1^F is the forward reaction rate in the first reaction, and C_{O_2} and C_{N_2} are the respective mass fractions of molecular oxygen and nitrogen Taking $C_{O_2} = 0\,235$ and $C_{N_2} = 0\,765$, evaluating k_1^F from Wray,[8] and using the equation of state gives

$$\omega_O/P\rho = 3\,58 \times 10^{16}(e^{-59\,400/T}/T^2) \qquad (1)$$

where T is in degrees Kelvin The variation of the oxygen atom mass fraction along the cone then becomes (neglecting diffusion)

$$C_O = (PX/V)[(3\,58 \times 10^{16})/T^2]e^{-59\,400/T} \qquad (2)$$

Next, it is assumed that a rapid exchange is achieved between the second and third reactions, whereby atomic nitrogen is consumed by the third reaction about as fast as it is produced by the second, giving

$$C_N = (17{,}170/T)C_O e^{-34\,480/T} \qquad (3)$$

and it is noted that both C_O and C_N vary linearly with PX/V at a fixed temperature

The ionization rate is obtained from the fourth reaction Neglecting reattachment, assuming a neutral plasma, and using Eqs (2) and (3) for the required atom concentrations,

$$\frac{\omega_{NO^+}}{P\rho} = \frac{2\,08 \times 10^{29}}{(T/1000)^{5\,5}}\left(\frac{PX}{V}\right)^2 e^{-185\,000/T} \qquad (4)$$

Integrating along the cone surface, the result

$$\frac{n_e}{P} = \frac{0\,7 \times 10^{22}}{T} C_{NO^+} = 0\,47 \times 10^{48} \frac{(PX/V)^3}{(T/1000)^{6\,5}} e^{-185\,000/T} \tag{5}$$

is obtained, giving the cubic law mentioned earlier

Equations (2) and (5) neglect diffusion and hold only when the gas is far out of equilibrium Before proceeding with the laminar boundary-layer analysis, it is interesting to compare this simplified kinetic model with results from an inviscid flow computer program of Wood et al [1] (Fig 2) The frozen temperature (vibrational equilibrium) was used in Eq (5) since it was found from the computer results that only as equilibrium was approached did dissociative cooling become appreciable Comparisons were made for several cone angles, freestream velocities, and altitudes (Fig 2)

Reasonably good agreement with the computer results was found over a wide range of conditions of interest However, Eq (5) begins to overpredict n/P near equilibrium Some improvement can be obtained if the frozen temperature in Eq (5) is reduced for dissociative cooling, as predicted by the formation of atomic species from Eq (2) Included in Fig 2 are the streamtube results for the peak electron densities in the laminar boundary layer As is to be expected, they correlate well with Eq (5) for the same frozen temperature, since both neglect diffusion

Laminar Boundary Layer

Assuming similarity[2] for the cone with a constant pressure P and wall temperature T_w, the continuity equation for the ith species becomes

$$\frac{l}{Sc_i} C_i'' + fC_i' + 2\frac{PX/3}{V}\left(\frac{\omega_i}{P\rho}\right) = 0 \tag{6}$$

where $l = \rho\mu/\rho_w\mu_w$, Sc_i is the Schmidt number (binary diffusion), f' is the velocity ratio, and the primes indicate differentiation with respect to the transformed normal coordinate η

Taking both l and Sc_i as known arbitrary constants enables the momentum and energy equations to be decoupled, and available solutions to be used for $f(\eta)$ and the static enthalpy For constant Prandtl number, the enthalpy can be tabulated in terms of $f'(\eta)$, e g , van Driest [9] The frozen temperature is found by neglecting the heat of formation (vibrational equilibrium), although, as will be demonstrated, it is possible to account for the heat of formation after the extent of dissociation has been determined

With $T(\eta)$ and therefore $\omega_i/P\rho(\eta)$ known, Eq (6) becomes a linear differential equation with variable, but known, coefficients Its solution by standard techniques, subject to the boundary conditions $C_i(0) = C_i(\infty) = 0$, gives

$$C_i = Sc_i\left(\frac{PX}{3V}\right)\left\{\frac{\int_0^\zeta F_{\zeta\zeta}^{Sc_i}\,d\zeta}{\int_0^\infty F_{\zeta\zeta}^{Sc_i}\,d\zeta} G(\infty) - G(\zeta)\right\} \tag{7}$$

where

$$G = \int_0^\zeta F_{\zeta\zeta}^{Sc_i}\,d\zeta_1 \int_0^{\zeta_1} \frac{\omega_i/P\rho}{F_{\zeta\zeta}^{Sc_i}}\,d\zeta_2$$

where $F(\zeta)$ is the incompressible Blasius function, and $\zeta = (2/l)^{1/2}\eta$

Equation (7) is integrated first for C_O The mass fraction C_N is then found from Eq (3) Equation (7) is then integrated a second time for C_{NO^+} and n/P Note that C_O and C_N vary linearly with PX/V, and n/P varies as $(PX/V)^3$ in the boundary layer, just as in the inviscid flow Since $n_e \sim P^4$, an extreme dependence, $n \sim \theta^8$, is found at a fixed temperature These scaling rules must be modified as equilibrium is approached

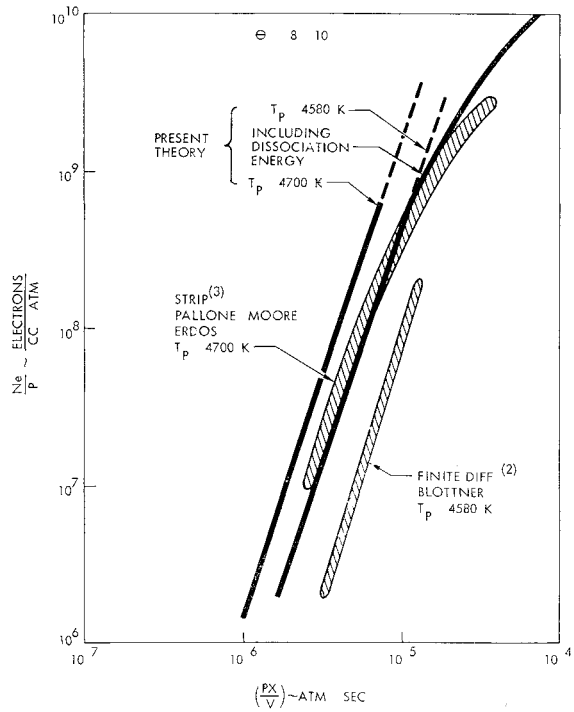

Fig 3 Comparison of present theory with more exact results

This procedure has been programmed on the 7090 Running time is about 1 min/case Although reasonable agreement with the theories[2 3] is found (Fig 3), caution should be attached to the absolute values, since approximate transport properties were used Thus, binary diffusion was assumed with $Sc_O = 0\,5$ An effective value for the ambipolar diffusion of the ion-electron pairs, $Sc_{NO^+_-} = 0\,25$, was used The value of l does not affect peak n/P, although it will change the boundary-layer thickness The reduction in n/P due to dissociative cooling is also shown and was obtained by accounting for the heat of dissociation of oxygen

The present analysis can be used to determine rapidly the effect of various parameters on the nonequilibrium electron concentration in viscous and inviscid flows It cannot replace exact solutions for final design In fact, an examination of exact results has suggested this simplified approach Finally, this analysis neglects the effects of entropy gradients, vibrational relaxation, and contamination due to injected species It is expected that all of these factors will tend to increase electron concentration levels

References

[1] Wood, A D Springfield, J F , and Pallone A J , Determination of the effects of chemical and vibrational relaxation on an inviscid hypersonic flow field," AIAA Conference on Physics of Entry into Planetary Atmospheres (August 1963)

[2] Lenard, M and Blottner, F , ' Finite rate plasma generation in the laminar air boundary layer of slender re-entry bodies," *Transactions of the Eighth Symposium on Ballistic Missile and Space Technology* (Defense Documentation Center, Alexandria, Va , 1963), Vol II, pp 3–33

[3] Pallone, A , Moore, J , and Erdos, J ' Nonequilibrium, nonsimilar solutions of the laminar boundary layer equations," Avco/RAD TM-63-58 (August 1963)

[4] DeRienzo, R , Wood A D Berner, F , and Teare, J D , "Effects of nonequilibrium on the hypersonic laminar air boundary layer," *Transactions of the Eighth Symposium on Ballistic Missile and Space Technology* (Defense Documentation Center, Alexandria, Va , 1963), Vol II, pp 35–64

[5] Blottner, F G , "Similar and nonsimilar solutions of the nonequilibrium laminar boundary layer" AIAA J 1, 2156–2157 (1963)

[6] Levinsky E and Fernandez F 'Approximate nonequilibrium air ionization in hypersonic flows over sharp cones," Aerospace Corp , TDR 269(S4810-60) 1 (November 7, 1963)

[7] Gibson, W F and Marrone, T V , "A similitude for nonequilibrium phenomena in hypersonic flight," AGARD Meeting on High Temperature Aspects of Hypersonic Fluid Dynamics, Brussels (March 1962)

[8] Wray, K L , "Chemical kinetics of high temperature air," *ARS Progress in Astronautics and Rocketry: Hypersonic Flow Research*, edited by F R Riddell (Academic Press Inc , New York, 1962), Vol 7, pp 181–204

[9] van Driest, E R , 'Investigation of laminar boundary layer in compressible fluids using the Crocco method," NACA TN 2597 (1952)

Finite Plane Deformation of a Thick-Walled Cylinder

M P Bieniek* and M Shinozuka†
Columbia University, New York, N Y

A HOLLOW cylinder of internal radius a and external radius b, bonded to a thin shell of thickness h and subject to internal pressure, is considered under the state of plane strain (Fig 1) The material of the cylinder is assumed to be nonlinear elastic solid with strain energy function of arbitrary form

The analysis of stresses and strains is performed under the assumption that the deformation of the cylinder is finite, i e , that the principal extensions, displacements, and displacement gradients are not small in comparison with unity

The general relations of the theory of finite deformations may be found, for example, in Refs 1–4 For the problem dealt with in this note, the cylindrical coordinates r, ϕ, and z are taken as the material coordinates $x^a (a = 1, 2, 3)$:

$$x^1 \equiv r \qquad x^2 \equiv \phi \qquad x^3 \equiv z \tag{1}$$

The spatial coordinates $\bar{x}^k (k = 1, 2, 3)$ are

$$\bar{x}^1 = \bar{r} = r + u \qquad \bar{x}^2 = \phi \qquad \bar{x}^3 = z \tag{2}$$

where u is the radial displacement

The covariant components of the material strain tensor can be expressed by

$$2\, e_{ab} = (u_{|b} + u_{b|a} + u_{|a}\, u_{|b}) \tag{3}$$

where the vertical bar denotes covariant differentiation, and summation is indicated by repeated indices For the present problem,

$$e_{11} = \frac{(\lambda_1^2 - 1)}{2} \qquad e_{22} = r^2 \frac{(\lambda_2^2 - 1)}{2} \qquad e_{33} = 0 \tag{4}$$

where $\lambda_1 = 1 + \partial u/\partial r$ and $\lambda_2 = 1 + u/r$ satisfying the compatibility condition

$$d\lambda_2/dr = (1/r)(\lambda_1 - \lambda_2) \tag{5}$$

The strain energy function W is a function of the three invariants of the material strain tensor of the form

$$J_1 = e_a{}^a \qquad J_2 = e_b{}^a e_a{}^b \qquad J_3 = e_b\, e^b e_a \tag{6}$$

Received November 13, 1963; revision received December 23, 1964 This research was supported by the Office of Naval Research under Contract Nonr 266(78)

* Associate Professor of Civil Engineering; presently Professor of Civil Engineering, University of Southern California, Los Angeles, Calif Member AIAA

† Assistant Professor of Civil Engineering

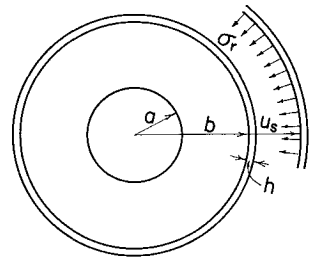

Fig 1 Thick-walled cylinder

The contravariant components of the spatial stress tensor can be expressed by

$$p^{kl} = J^{-1} \frac{\partial W}{\partial e_{ab}} \frac{\partial \bar{x}^k}{\partial x^a} \frac{\partial \bar{x}^l}{\partial x^b} \tag{7}$$

where $J = det|\, \delta_b{}^a + u^a{}_{|\,b}\,| = \lambda_1\lambda_2$ for the present problem and the deformation gradients $\partial \bar{x}^k/\partial x^a$ follow immediately from Eqs (1) and (2)

The physical components of stress σ_{kl} can be given in terms of p^{kl} as follows:

$$\begin{aligned} \sigma_{11} \equiv \sigma_r &= p^{11} = \lambda_1\lambda_2{}^{-1} W_1 \\ \sigma_{22} \equiv \sigma_\theta &= \bar{r}^2 p^{22} = r^2 \lambda_1{}^{-1}\lambda_2 W_2 \\ \sigma_{33} \equiv \sigma_z &= p^{33} = \lambda_1{}^{-1}\lambda_2{}^{-1} W_3 \end{aligned} \tag{8}$$

where the quantities $W_a = \partial W/\partial e_{aa}$ (no summation on a) are equal to the corresponding components of the material stress tensor [1]

The equations of equilibrium in terms of the strain-energy function W are

$$\frac{\partial W}{\partial e_{ab}} (\delta_b + u_b)_{|a} = 0 \tag{9}$$

For the problem under consideration, there is only one nontrivial equation of equilibrium, which is, after some manipulation, obtained from Eq (9) in the form

$$\frac{d}{dr}(W_1\lambda_1) + \frac{1}{r} W_1\lambda_1 - rW_2\lambda_2 = 0 \tag{10}$$

Performing the differentiation with respect to r and substituting Eq (5), Eq (10) is solved for $d\lambda_1/dr$:

$$\frac{d\lambda_1}{dr} = -\left(\frac{\partial W_1}{\partial \lambda_1}\lambda_1 + W_1\right)^{-1} \times \left[\frac{\partial W_1}{\partial \lambda_2}\frac{1}{r}(\lambda_1 - \lambda_2)\lambda_1 + \frac{1}{r} W_1\lambda_1 - rW_2\lambda_2\right] \tag{11}$$

Equations (5) and (11) represent a system of two differential equations well suited for numerical analysis These equations are easily integrated for λ_1 and λ_2 with the aid of an electronic digital computer The two conditions at $r = b$ which determine the initial values of λ_1 and λ_2 are obtained by prescribing the radial displacement of the shell u and by computing the corresponding pressure on the shell (Fig 1) Since the deformation of the shell is smaller than the deformations in the cylinder and can be assumed to be infinitesimal, the approximate value of the hoop stress σ in the shell is $\sigma = E\,u/b(1 - \nu^2)$; hence the pressure p on the intersurface between the shell and the cylinder is

$$p = \frac{E_s}{1 - \nu^2}\frac{h}{b}\frac{u_s}{b + u} \tag{12}$$

where E and ν are Young modulus and Poisson ratio of the shell

Thus the two conditions at $r = b$ are

$$\lambda_2 = 1 + u/b \tag{13}$$